Adams *et al. Progress in Earth and Planetary Science* (2015) 2:29
DOI 10.1186/s40645-015-0058-1

Progress in Earth and Planetary Science
a SpringerOpen Journal

REVIEW Open Access

Liquid sodium models of the Earth's core

Matthew M. Adams[1*], Douglas R. Stone[1], Daniel S. Zimmerman[4] and Daniel P. Lathrop[2,3]

Abstract

Our understanding of the dynamics of the Earth's core can be advanced by a combination of observation, experiments, and simulations. A crucial aspect of the core is the interplay between the flow of the conducting liquid and the magnetic field this flow sustains via dynamo action. This non-linear interaction, and the presence of turbulence in the flow, precludes direct numerical simulation of the system with realistic turbulence. Thus, in addition to simulations and observations (both seismological and geomagnetic), experiments can contribute insight into the core dynamics. Liquid sodium laboratory experiments can serve as models of the Earth's core with the key ingredients of conducting fluid, turbulent flow, and overall rotation, and can also approximate the geometry of the core. By accessing regions of parameter space inaccessible to numerical studies, experiments can benchmark simulations and reveal phenomena relevant to the Earth's core and other planetary cores. This review focuses on the particular contribution of liquid sodium spherical Couette devices to this subject matter.

Keywords: Magnetic dynamos; Fluid experiments; Geodynamo; Magnetic induction; Zonal flows; Turbulence; Experimental fluid dynamos; Spherical Couette flow

Review

Introduction

Large-scale magnetic fields are common in the universe and are found in planets, stars, accretion disks, and galaxies. Many of these fields are thought to be the result of self-sustaining dynamo action, whereby motions of a conductive fluid in the presence of a magnetic field give rise to induced currents that in turn generate magnetic fields that reinforce the original field (Larmor 1919; see also, e.g., Rüdiger and Hollerbach 2004). Starting from an arbitrarily small field, the flow of a conductive fluid, driven by some energy source, can result in a persistent large-scale magnetic field that can also show a variety of dynamical changes including polarity reversals. In our own solar system, the Sun, a majority of the planets (Mercury, Earth, Jupiter, Saturn, Uranus, Neptune (see, e.g., section 2.9 in Rüdiger and Hollerbach 2004)), and at least some moons (e.g., the Jovian moon Ganymede (Kivelson et al. 1996)) exhibit dynamos, while the Earth's Moon (Garrick-Bethel et al. 2009) and Mars (Acuña et al. 1999) show signs of past dynamo action. Farther out, most stars generally have magnetic fields that are thought to arise via dynamo action, and the galaxy itself has a magnetic field that may also be the result of this mechanism (Rüdiger and Hollerbach 2004).

The prevalence of such large-scale fields implies that this mechanism of dynamo action is robust, generally having three ingredients: a large volume of conductive fluid, an energy source to drive the dynamo, and overall rotation to help organize the flow (see, e.g., Olson 2013). The first requirement can be fulfilled by the large liquid metal cores of planets, including Earth with its liquid iron outer core and Jupiter with its liquid metallic hydrogen core, by the plasma found in stars including the Sun, and by conductive aqueous solutions, such as those found in Uranus and Neptune (see, e.g., Rüdiger and Hollerbach 2004). The second requirement, needed to sustain the magnetic fields against the inevitable Ohmic dissipation resulting from the finite conductivity of the fluid, can be met by a variety of sources, including convection driven by thermal or compositional gradients, as well as precessional and tidal forcings in planetary bodies. The third ingredient, rotation, while not necessary in all cases, is often helpful in organizing the feedback between the flow and the magnetic field. Given that the conservation of angular momentum results in most stars and planetary bodies having a significant amount of overall rotation, rotational effects will often be present even in dynamos

*Correspondence: madams13@umd.edu
[1] Institute for Research in Electronics and Applied Physics, University of Maryland, College Park, 20742 MD, USA
Full list of author information is available at the end of the article

not requiring them for their operation (Olson 2013). In addition, for rapidly rotating systems such as planetary bodies, the interaction of magnetic fields with convection can result in the possibility of distinct weak- and strong-field regimes (see, e.g., section 2.3.3 of Rüdiger and Hollerbach 2004), possibly of relevance to the dynamics of the geodynamo and of other planetary dynamos.

While nature apparently has no problem generating dynamos, they have proven more elusive in laboratory settings. Thus far, all fluid dynamos realized in a lab have either involved imposing a specific flow pattern via an arrangement of pipes and baffles (as in the experiments in Riga (Gailitis et al. 2000, 2001, and 2008) and Karlsruhe (Stieglitz and Müller 2001)) or have had ferromagnetic boundaries as a necessary ingredient (as in the von Kármán sodium (VKS) experiment (Monchaux et al. 2007; Berhanu et al. 2007)). Significant research in numerical dynamos has been performed, including simulations of the geodynamo that exhibit a dipolar structure and occasional polarity reversals (Glatzmaier and Roberts 1995; Takahashi et al. 2005), but these geodynamo simulations use one or more unrealistic diffusive parameters in modeling planetary or stellar dynamos.

Both the computational and the experimental difficulties in modeling an Earth-like (or other planetary or stellar) dynamo can be understood in terms of dimensionless parameters. Such parameters are generally constructed by making non-dimensional the applicable equations of motion, such as the Navier-Stokes equation. They may be understood as quantifying the relative importance or strength of various forces. Very large or very small dimensionless parameters indicate that a wide range of length and time scales may be important. A particularly noteworthy example of this is turbulence, whereby a fluid exhibits complicated dynamics on a wide range of length and time scales, which must all be resolved if the flow is to be directly simulated by numerical computations. Similarly, for an experimental device to be a good analog of a planetary core, it must match as many of the applicable dimensionless parameters as possible. In both cases, some of the relevant dimensionless parameters are beyond those achievable in simulations and laboratory experiments (see Table 1).

Although both simulations and experiments fall short of the parameter regimes found in planetary and stellar dynamos, experiments can get closer than simulations in certain cases. In particular, turbulent flows are readily achieved in the laboratory that are not amenable to direct numerical simulations. On the other hand, simulations have the advantage of having measurement access to all properties of a fluid flow, unlike experiments which are generally constrained to a limited number of local measurements and perhaps a few global measurements. Simulations can also arbitrarily vary material properties, where again experiments are limited by the available working fluids. Thus, dynamo studies can be furthered through a combination of observational, experimental, and computational efforts.

This review describes the contribution of liquid sodium spherical Couette devices to dynamo studies and aims to give an overview of the interplay between experiments, simulations, and observations. First, dimensionless parameters are discussed, allowing comparison of these three approaches. Then, some observational data are discussed, which motivates the experimental and numerical studies considered in the next two sections. We conclude with some speculations about the potential for data assimilation to further integrate these approaches to understanding dynamo action.

Dimensionless parameters

As noted above, dimensionless parameters allow comparison of observational, experimental, and computational results. The definitions and values of some dimensionless parameters relevant to the experiments and simulations to be discussed can be found in Table 1. Of particular interest in dynamo studies are the Reynolds number, $\mathrm{Re} = UL/\nu$, and the magnetic Reynolds number, $\mathrm{Rm} = UL/\eta$. Here, U and L represent velocity and length scales of the flow, respectively, while ν and η are the kinematic viscosity and magnetic diffusivity, respectively. The Reynolds number characterizes the presence and strength of turbulence in the flow. Above some critical value for Re, a flow will transition from laminar flow to turbulence, and above this value, a larger Re implies stronger turbulence. Re can also be viewed as a ratio between inertial forces

Table 1 Dimensionless parameters. Typical values for experiments and simulations, along with estimated values for the Earth's core. Values for the Earth's core from Olson (2013)

Parameter	Symbol	Definition	Experiments	Simulations	Earth's outer core
Magnetic Prandtl number	Pm	ν/η	$<10^{-5}$	$> 10^{-3}$	10^{-5}
Reynolds number	Re	UL/ν	$<10^{8}$	$<10^{6}$	10^{8}
Magnetic Reynolds number	Rm	UL/η	$<10^{3}$	$<10^{4}$	300–1000
Rossby number	Ro	$\Delta\Omega/\Omega$	$>10^{-5}$	$>10^{-5}$	10^{-5}
Ekman number	E	$\nu/\Omega L^2$	$>10^{-8}$	$>10^{-6}$	10^{-14}

(causing advection and vortex stretching in the flow) and viscous forces (smoothing out variations in velocity). Similarly, the magnetic Reynolds number, Rm, can be viewed as the ratio between advection of the magnetic field, tending to strengthen it via stretching of magnetic field lines, and dissipation of the field via diffusion due to resistive losses. The higher the Rm of a flow, the more likely dynamo action is to occur. For a given flow that is capable of dynamo action, a self-sustaining field will arise if Rm exceeds some critical value. In general, this critical value is unknown, however, so experiments simply try to maximize it, and the estimated values for astronomical bodies provide some guidance as to what values may be necessary in a given configuration. Also, since rotation is often an important ingredient in both planetary dynamos and in experiments, the Ekman number $E = \nu/\left(\Omega L^2\right)$ is relevant. This parameter quantifies the relative strength of viscous and rotational effects and also sets the size of the Ekman boundary layer, which scales as $E^{1/2}$.

Experiments and simulations can reach Rm values comparable to those of magnetized planetary bodies, consistent with the fact that dynamos have been realized in both experiments and simulations. While experiments can also reach realistic values of Re, simulations cannot resolve the wide range of length and time scales needed to capture such turbulent flows, and thus, simulations generally introduce unrealistically large viscosities in order to suppress turbulence and render the flow amenable to simulation (see Fig. 1). Finally, in the case of the Ekman number, astrophysical bodies often exhibit values well beyond the range of both experiments and simulations (though again experiments can go to lower values than simulations and thus get closer to values typical of planetary and stellar bodies).

Another set of dimensionless parameters involves the strength of the magnetic field. In studies of kinematic dynamos, where the background magnetic field is generally assumed to be negligible, such parameters will not be relevant. However, such parameters are important for characterizing dynamo systems once a magnetic field has been established. They may also be relevant to the description of subcritical dynamos, for which an initial finite field strength is required for dynamo action to occur, though no external field is required to sustain

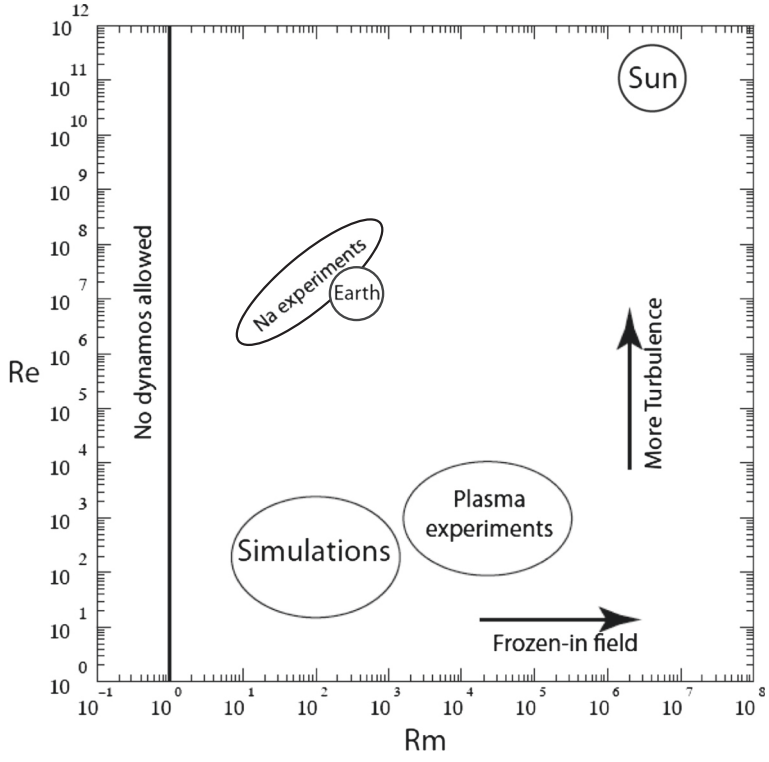

Fig. 1 Parameter space. A map of the Rm-Re parameter space. Note that sodium experiments operate at a magnetic Prandtl number (Pm) of $\sim 7.5 \times 10^{-6}$ and therefore fall around a line in this space. The Earth's quoted values of Rm = 300–1000 in Table 1 are based on the estimates for a range of scales of motion in the outer core (see Olson 2013 for details). Also, the estimate of Pm for the Earth ($\leq 10^{-5}$) has a large uncertainty, contributing to the spread in possible values for the Earth in this parameter space, represented schematically by a circle. Note that sodium experiments can achieve Earth-like values for these parameters. Simulations are confined to much lower Re (or, equivalently, much larger Pm for similar values of Rm)

the dynamo action once it is established. Since to date dynamos have only been achieved under a limited number of laboratory settings, systems that have relatively strong external applied fields are also often used to study hydromagnetic processes. Dimensionless parameters relevant to such studies include the Elsasser number and the interaction parameter. The Elsasser number $\Lambda = B_0^2/(\Omega\mu_0\rho\eta)$ measures the ratio of Lorentz to Coriolis forces; here, μ_0 is the permeability of free space, ρ is the fluid density, B_0 is the applied magnetic field, and the other symbols are as above. It thus quantifies the relative importance of the magnetic field and overall system rotation in influencing the fluid flow. The interaction parameter $N = \sigma L B_0^2/\rho U$, where σ is the conductivity of the fluid, provides the ratio of Lorentz forces to inertial forces in the system. For small N, Lorentz forces do not appreciably affect the flow, while for large N, the Lorentz forces can significantly modify the flow.

Observations

A primary motivation of dynamo studies is to understand how various astrophysical bodies, including the Earth and the Sun, generate their magnetic fields. Historical observations of sunspots and global models of the Earth's magnetic field are available for the past few hundred years, giving a sense of the dynamics of both bodies in that time period (Eddy 1978; Jackson et al. 2000). In the satellite era, much more refined measurements are available for both bodies, though these data are limited to a timespan of decades. These include satellite measurements of the Earth's field as well as X-ray observations of the Sun, giving more detailed information about the magnetic activity in its corona (see, e.g., resp. Langel 1993; Sams et al. 1992). Finally, measurements of remanent magnetization of rocks in the Earth's crust provide crude information about the Earth's magnetic field extending back hundreds of millions of years.

These data provide a portrait of a dynamic magnetic field for both the Sun and the Earth. Sunspots (the sites of intense magnetic fields) undergo regular variations in number and spatial distribution during the 11-year solar cycle (or 22 years to return to the same polarities). Moreover, the sunspot number has shown significant variations during historical times, including the Maunder minimum when very few sunspots were observed for an extended period. Similarly, rock records on Earth reveal a series of polarity reversals, with a wide range of spacings, and historical records show smaller variations in the Earth's field on much shorter time scales (see, e.g., Merrill et al. 1996 for a discussion of these various findings).

In addition to the observations of the magnetic fields of these bodies, other investigations, observational as well as experimental and computational, have greatly improved the theoretical understanding of both bodies. In particular, seismological studies of the Earth and helioseismological studies of the Sun have provided knowledge of the structure of their interiors, which can then be combined with experimental and numerical investigations of material properties. This in turn allows improved estimation of relevant dimensionless parameters.

Experiments

In trying to understand the geodynamo in particular, a class of experimental and numerical studies have focused on spherical Couette flow (see Chp. 7 of Rüdiger et al. 2013 for an excellent overview). This consists of flow in the space between an outer bounding spherical shell and a concentric inner sphere of smaller diameter. Flow is driven by differential rotation between the inner and outer spheres. The system can be characterized by the difference in inner and outer rotation rates $\Delta\Omega$ and, if the outer sphere is rotating, by the overall system rotation Ω (i.e., the outer sphere rotation rate). Such systems are geophysically relevant, having a similar geometry to the Earth's core, especially if they approximately match the inner-to-outer core radius ratio of 0.35. While not capturing all aspects of the geodynamo, such systems are relatively simple models of dynamo action, providing a straightforward way to achieve the differential rotation that is a key ingredient of many dynamo mechanisms (see, e.g., Wei et al. 2012).

A significant difference between flow in the Earth's core and such a setup is the driving of the flow. The Earth's core flows (including any differential rotation contributing to dynamo action) are believed to be driven primarily by a combination of compositional and thermal convection, with rotational, and possibly precessional, effects playing a significant role. In spherical Couette flows, on the other hand, a shear flow is driven by differential rotation imposed at the boundaries. Thus, the angular momentum transport between the two spheres, rather than heat and chemical transport, is the driver of the flow.

While thermal convection can be used to drive flows in experimental devices, these flows tend to be less vigorous than shear flows, as measured by the achievable Re and Rm. Moreover, if hydromagnetic phenomena are to be investigated, the working fluid must be a conductor, and a good electrical conductor is desirable to achieve a large Rm. Thus, experiments generally make use of a liquid metal, like sodium or gallium. In fact, liquid sodium is the best liquid conductor usable in such experiments, but with high electrical conductivity comes high thermal conductivity. Thus, when a thermal gradient is used to drive flows in liquid sodium, the induced flows are relatively weak, resulting in a low Re and thus, since $\mathrm{Rm} = \mathrm{RePm}$, a relatively low Rm (at least compared to shear-driven sodium flows). For instance, the rotating convection experiment described in Shew and Lathrop

(2005) achieved an Re of ∼40,000 based on zonal flows in the liquid sodium; later, it was reconfigured to be a mechanically driven spherical Couette device, achieving Re of $\sim 10^6$ (Kelley 2009). Spherical Couette devices using liquid sodium can thus achieve turbulent hydromagnetic flows with significant rotational effects in an Earth-like geometry. A similar experimental setup is that of a spherical vessel of fluid with flow driven by impellers; while less Earth-like, the impellers allow more vigorous flow to be driven as compared to the smooth-walled boundaries of spherical Couette devices.

A number of liquid sodium devices have been implemented with a spherical geometry. The Madison dynamo experiment (MDE) is an example of an impeller-driven flow (Nornberg et al. 2006), while the Derviche Tourneur Sodium (DTS) experiment in Grenoble is a spherical Couette device with a ferromagnetic inner sphere (Nataf et al. 2006, 2008). At the University of Maryland, a series of liquid sodium devices have been constructed, including three spherical vessels ranging in size from 30 cm to 3 m. The two current sodium experiments are both spherical Couette devices, 60 cm and 3 m in diameter, and magnetic fields can be applied to the fluid volume using external coils. In spherical geometries, we note that both magnetic and velocity fields are commonly described using vector spherical harmonics to decompose the fields into poloidal and toroidal components (see Bullard and Gellman 1954). This can always be done for magnetic fields which are always divergence-free and can also be done for the velocity field of an incompressible flow—such as that found in liquid metal experiments. The toroidal component of the magnetic field has no radial component and does not extend out of the conductor; thus, for measurements outside the Earth's core (or outside the fluid volume of an experiment), only the poloidal component of the field can be measured, which can be written as the gradient of a scalar field (assuming no other current sources). Models of the Earth's field outside its core are often expanded in terms of spherical harmonics, with the coefficients in the expansion (one for each harmonic, identified by degree l and order m) referred to as Gauss coefficients (after Gauss, the first to represent the Earth's field in this manner (Gauss 1839)). Moreover, descriptions of the dynamo mechanism are often conceptualized in terms of the conversion of poloidal field into toroidal field (the ω effect) and of toroidal field into poloidal field (the α effect) via fluid flow.

Below, we first review some of the results from previous successful dynamo experiments (all in non-spherical geometry), along with some results from MDE, which while not a dynamo shares many characteristics with the VKS experiment (the only successful dynamo in an open geometry). Then, we review some results from the DTS experiment, a liquid sodium device modeled on the Earth's core and having a strong imposed dipolar field. This section closes with discussion of the Maryland spherical Couette experiments.

Previous dynamos and the Madison dynamo experiment

While the Maryland devices and DTS are modeled on the Earth's core, MDE follows in the tradition of the Riga and Karlsruhe dynamos in being based on a kinematic dynamo (Riga: the Ponomarenko flow (Ponomarenko 1973); Karslruhe: G.O. Roberts flow (Roberts 1972)). While the mean flow of the device approximately models a laminar kinematic dynamo, turbulent fluctuations are always present as well. In the Riga and Karlsruhe dynamos, turbulent fluctuations were limited in size by the diameter of the pipes used in constraining the flow, thus separating the scale of the turbulent eddies from the system size over which the dynamo acts. MDE, on the other hand, has an open geometry like VKS and the Maryland devices where turbulent fluctuations can be present up to the system size. Such a geometry is more astrophysically relevant, since natural bodies generally have unconstrained flows in simply connected regions more akin to those of MDE or VKS than the Riga or Karlsruhe dynamos (see, e.g., Nornberg et al. 2006). The lack of scale separation also means, however, that the predictions of laminar kinematic dynamo theory, while still a potentially helpful guide, are no longer reliable.

The Madison dynamo experiment (MDE) has a very similar driving setup to that of the VKS experiment, but in a spherical rather than cylindrical container. The experiment consists of a 1 m diameter spherical shell filled with liquid sodium, driven by two impellers. The impellers have a common axis, mounted on shafts entering the container from the two poles of the experiment. Two sets of coil pairs, one coaxial with the impellers and one perpendicular to the axis, can be used to apply a magnetic field of dipolar or quadrupolar symmetry, either parallel to the impeller rotation axis or perpendicular to it. Unlike the VKS experiment, MDE does not achieve dynamo action, including when using ferromagnetic impellers (Nornberg et al. 2014a). While no dynamo was seen, a variety of phenomena involving the interaction of turbulent flow with magnetic fields have been observed and quantified.

As noted above, the setup of MDE was in part motivated by a kinematic dynamo for the spherical geometry. This flow consists of counter-rotating toroidal flows in the two hemispheres (driven by the counter-rotating impellers), as well as poloidal rolls consisting of outflow from the equatorial regions between the impellers towards the poles (again driven by the impellers) and a return flow along the outer boundary (Nornberg et al. 2006). This double-vortex flow results in a kinematic dynamo in the laminar case (Dudley and James 1989), with feedback resulting in a transverse dipole (i.e., a dipole oriented perpendicular

to the axis defined by the impeller shafts). Using liquid sodium, with the resulting small Pm, however, means that the actual experiment will be highly turbulent, with Re $\sim 10^7$ and turbulent fluctuations up to $\sim$20 % of the mean (Spence et al. 2006).

While the mean flow of MDE is expected to approximate that of the laminar kinematic dynamo, these turbulent fluctuations in the experiment can have a number of effects. Nornberg et al. (2006) follow a mean-field approach in separating the magnetic and velocity fields into their mean and fluctuating components and focusing on the mean field and the net effect of the fluctuating components on it (see, e.g., Krause and Rädler 1980). Then, the expected dynamics are the sum of that due to the mean, axisymmetric flow (approximating the laminar kinematic dynamo) and the net effect of the fluctuations in the velocity and magnetic fields (due to turbulence). Correlated fluctuations in the magnetic and velocity fields can result in coherent generation of magnetic field (referred to as the α effect, first experimentally observed by Steenbeck et al. 1968). Tangling of the magnetic field lines by turbulent eddies can result in an increase in dissipation of magnetic field in the system, which can be viewed as a turbulent enhancement of the system's magnetic diffusivity (termed the β effect). Finally, gradients in the amount of turbulence can result in flux expulsion from regions of higher turbulence (the γ effect).

In the parameter regimes studied, the experiment does not achieve dynamo action, but by applying magnetic fields in a number of different geometries, the effects of turbulent fluctuations have been investigated. For the case of an axial applied field, in addition to the expected induced field due to the mean flow (axisymmetric $l = 3$ and $l = 5$ modes), an axial dipole is also seen (Spence et al. 2006). This cannot be due to the interaction of the axisymmetric mean flow with the axisymmetric applied field (by well-known symmetry arguments, see Cowling (1934)), so it is argued that it must be due to a turbulent electromotive force (EMF) which breaks the symmetry of the system.

In addition to the liquid sodium experiment, the Madison group has an identical-scale water experiment, which when run at an appropriate temperature (40 °C), approximately matches the kinematic properties of liquid sodium (see, e.g., Nornberg et al. 2006). In the water experiment, laser Doppler velocimetry (LDV) measurements of the velocity were taken (which are not possible in opaque liquid sodium), allowing the mean flow field in the sodium experiment to be determined. By comparing the induced magnetic field in the liquid sodium to the field expected by the action of this mean flow field on the applied magnetic field, Spence et al. (2007) infer the presence of electrical currents in the experiment due to the turbulent EMF. This current in turn produces poloidal (which is primarily dipolar) and toroidal field that is opposed to the primary field induced by the mean flow; the system exhibits turbulent diamagnetism. Kaplan et al. (2011) report on the results of installing equatorial baffles in MDE, resulting in a reduction of the global β effect in the experiment. Further improvement in reducing the turbulent resistivity were reported in Nornberg et al. (2014), though the system was still below the threshold for a dynamo.

In addition to these relatively steady effects, intermittent bursts of magnetic field have also been observed in MDE (Nornberg et al. 2006a). When an axial magnetic field is applied to the experiment, a fluctuating amount of energy is observed in the transverse dipole, which is the least-damped magnetic eigenmode predicted by laminar kinematic dynamo theory. The orientation of the dipole within the equatorial plane of the experiment is random, so on average the induced magnetic field is axisymmetric. Also, the distribution of the strength of magnetic fluctuations diverges from a Gaussian distribution due to these large bursts, serving as another indication that the bursts are not simply due to noise in the system. The strength of the Lorentz forces due to the bursting field is at most comparable to those due to the applied field, so the interaction parameter remains low ($N \sim 0.01$), and the effect of these forces is minimal.

The authors propose several possible explanations for these bursts. Turbulent velocity fluctuations could lead to a locally higher Rm, resulting in it temporarily exceeding the critical Rm for this least-damped eigenmode. Alternatively, the turbulent fluctuations could alter the overall shape of the flow, making it more favorable to this eigenmode, effectively reducing the critical Rm for it below the experiment's Rm (again, temporarily). In either case, the mode would start growing, and there would be a burst of magnetic field in the form of a transverse dipole, which would decay away once the favorable turbulent fluctuations had dissipated. Another possibility is that if at small scales the kinetic helicity of eddies becomes strong enough, the current produced by their interaction with the applied field could result in the bursts. In summary, the authors argue that for a turbulent dynamo the transition from non-dynamo to dynamo states will be marked not by a smooth transition from a decaying to a growing magnetic eigenmode (as in laminar kinematic dynamos), but rather by intermittent bursts of magnetic field.

The Derviche Tourneur Sodium experiment: the magnetostrophic regime

The DTS experiment was designed to study the magnetostrophic regime relevant to the Earth's core (see, e.g., Cardin et al. 2002). In this regime, the Coriolis and Lorentz forces dominate viscous forces. Such a regime is characteristic of rapidly rotating systems with strong magnetic fields. The DTS experiment has a 42 cm outer

diameter sphere, while the 14.8 cm inner sphere has a copper surface with an internal permanent magnet, so that a dipolar field is applied to the liquid sodium that fills the gap between the inner sphere and the outer spherical shell. The dipole is oriented along the axis of rotation of the spheres. The inner and outer spheres can be rotated independently, driving a variety of flows that are significantly modified from the hydrodynamic case by the presence of the relatively strong field of the inner sphere.

In terms of dimensionless parameters, such a system has a small Ekman number (so rotational effects dominate viscous ones) and an Elsasser number $\Lambda \sim O(1)$, so that the Coriolis and Lorentz forces are of comparable strength. Although laboratory experiments cannot reach Ekman numbers comparable to those found in planets and stars, they are capable of reaching regimes of rapid rotation that are computationally inaccessible. Since a dynamo has not yet been demonstrated in the spherical geometry, however, in order to reach an Elsasser number of order $\sim O(1)$, some other magnetic field must be applied to the fluid. In the case of DTS, the inner sphere is ferromagnetic, applying a dipolar field of fixed strength. Given this geometry, a variety of force balances are present in the experiment, ranging from a magnetically dominated one near the inner sphere to a rotationally dominated one near the outer sphere (see, e.g., Nataf et al. 2006). For instance, magneto-coriolis waves have also been observed, where both rotational effects (via the Coriolis force) and magnetic effects result in the fluid supporting novel wave modes (Schmitt et al. 2013).

Another such flow involves the super-rotation of the flow as compared to the inner sphere, so that the flow velocity exceeds that of both system boundaries (Brito et al. 2011). Super-rotation was first found in numerical simulations (Starchenko 1997; Dormy et al. 1998) and was later found in the DTS experiment (Nataf et al. 2006, 2008, and Brito et al. 2011). In Nataf et al. (2006, 2008), the azimuthal angular velocities of the flow were inferred from electric potential measurements at the surface of the outer sphere and interpreted as revealing a strong super-rotation of the liquid sodium in the equatorial region.

While super-rotation was found, consistent with the previous numerical predictions, there were also notable differences between the numerical model and the experimental results. In particular, the experimental variation of the electric potential with latitude did not match that of the numerical simulation, and oscillatory motion near the equator of the outer sphere, seen using ultrasound Doppler velocimetry (UDV), did not match up with the steady result in numerics. The oscillations were interpreted as due to an instability of the super-rotating region.

Intuitively, this phenomenon can be understood in terms of the electric currents in the system and the geometry of the applied field lines (see discussion of simulation results below and Hollerbach (2001)). Generally, the electric currents follow the field lines, thus generating no Lorentz force on the fluid. In boundary layers, the electric currents cross field lines, generating Lorentz forces that balance the viscous forces. Near the equator of the experiment, however, given the dipole geometry of the applied field, if large enough currents are flowing, they are forced to cross the magnetic field lines here. The Lorentz forces that result allow the inner sphere to act like a magnetic propeller, grabbing on to the fluid and forcing it to spin with it rather than with the outer sphere.

These forces can become so large that they overcompensate for the viscous forces due to the differential rotation of the inner with the outer sphere and result in the acceleration of the fluid in this region to angular velocities that exceed that of the inner sphere. In Brito et al. (2011), UDV measurements confirmed the presence of super-rotating jets in DTS for the case of a stationary outer sphere. They also show that the electric potential measurements are somewhat difficult to interpret and are not always a good guide to the azimuthal velocities. The phenomenon of super-rotation is an interesting and unusual hydromagnetic phenomenon, and comparison with numerical models allows elucidation of the limits of linear models and may shed light on why Earth-like geodynamo models do surprisingly well (Brito et al. 2011).

Another experimental result from DTS is of particular interest for dynamo studies. Cabanes et al. (2014a) report on measurements of the α and β effects and note that the β effect due to small-scale turbulent fluctuations is negative in the interior of the experiment and positive closer to the outer sphere. Thus, the turbulent fluctuations near the inner sphere reduce the effective magnetic diffusivity, implying that turbulence could be a contributing factor to dynamo action, as opposed to a hindrance (as it has often seemed in past experiments). Indeed, the authors speculate that if the magnitude of this negative β effect were to grow large enough, it could promote dynamo action. As reported in another paper (Cabanes et al. 2014), the ω effect is present in the rotationally dominated outer region, which is another possible ingredient of dynamo action.

Spherical Couette experiments at the University of Maryland

At the University of Maryland, a series of liquid sodium devices have been constructed. A device with a 30 cm stationary outer spherical shell had flows driven by impellers, propellers, or an inner sphere (Sisan et al. 2004). A larger 60 cm device was originally constructed as a rotating convection experiment, with a cooled inner sphere and a heated outer spherical shell driving flows in liquid sodium, with the centrifugal force due to the overall system rotation standing in for gravity (Shew and Lathrop 2005). As mentioned above, the high thermal conductivity

of sodium makes it difficult to achieve vigorous flows with a thermal gradient, so this device was modified to have a differentially rotating inner sphere (Kelly et al. 2006, 2007, 2010). Finally, the 3 m device is a spherical Couette device that was initially run as a water experiment but is now operating with liquid sodium (see Figs. 2 and 3) (see, e.g., Zimmerman 2010 and Zimmerman et al. 2014).

While the water experiments in the 3 m device were initially for mechanical debugging purposes in preparation for the sodium experiments, they provided some new results for the case of non-magnetic spherical Couette flow. In these experiments, the two variables are the rotation rates of the inner and outer sphere. Using dimensionless parameters, this parameter space can be characterized by Ro and Re. In water, the primary measurements were the torque required to drive the inner sphere (from a reaction flange torque sensor), pressure measurements, and wall-shear and UDV measurements. It was found that Ro determines the state of the flow, while varying Re just scales the velocities and torques seen. For some Ro values, moreover, it was found that the system exhibited bistability, switching between two distinct states as determined by the torque required to drive the inner sphere at its rotation rate (Zimmerman et al. 2011). The torque was significantly higher in one state (the high torque state) as compared to the other (the low torque state).

Fig. 2 Rendering of the 3 m experiment. The inner sphere and the outer spherical shell can be driven independently by their two respective motors (*top*). Liquid sodium serves as the working fluid for hydromagnetic experiments

This state was also investigated in liquid sodium with the 60 cm device (see Fig. 4). For these experiments, an array of Hall probes measured the magnetic field outside the outer sphere, while the motor drives provided coarse-grained torque measurements. A relatively weak applied field allowed the velocity profile in the device to be inferred from induced field measurements. First, the induced field is modeled as a sum of vector spherical harmonics up to degree and order 4. These Gauss coefficients are found via a least squares fit to the field measurements. Selection rules can be used to determine the possible patterns of fluid flow in the device, since the applied field geometry is known (see, e.g., Sisan 2004). From the magnetic field measurements, the presence of an inertial wave was identified, consistent with results in the 3 m device. In addition, the presence of power in another Gauss coefficient correlated well with the low-torque state and has been interpreted as the result of interaction of the Earth's field (which is not shielded out in the device) with a Rossby wave. This wave is nearly 2D and given its geometry would not be expected to cause any induction at all when acted on by a uniform, axially-aligned field like the one applied in the experiment.

While the results from the 60 cm device are generally compatible with those from 3 m, a significant difference is found in the values of Ro for which the bistable states occur. This may be due to geometric differences between the two devices: the 60 cm device has a relatively thicker shaft which spins with the outer sphere, as opposed to the shaft in 3 m that spins with the inner sphere. Thus, at least in this case, analogous states can be found despite significant geometric differences in the devices, with the 60 cm device requiring a larger Ro, and thus faster relative inner rotation, which intuitively might be thought of as being necessary to overcome the effect of the large shaft rotating with the outer sphere (Zimmerman 2010).

In addition to regions of bistability, the 3 m water experiments also revealed the presence of precession-driven flows (Triana et al. 2012). When the inner and outer spheres are locked together and spun up to some constant rotation rate, one might expect the flow to come to a state of solid body rotation with the spheres. However, the laboratory is not an inertial frame since the Earth is rotating. Thus, the axis of the experiment is precessing, completing one revolution a day. This precession of the experiment's rotation axis drives the spin-over mode, which can be understood as the fluid spinning in a state of solid-body rotation but with an axis that lags that of the experiment itself. Effectively, the fluid retains some "memory" of the previous orientations of the rotation axis. The structure and strength of the observed flows were consistent with the presence of a spin-over mode driven by precession. Since many planetary bodies, including the Earth, exhibit significant amounts of precession of their rotation axes,

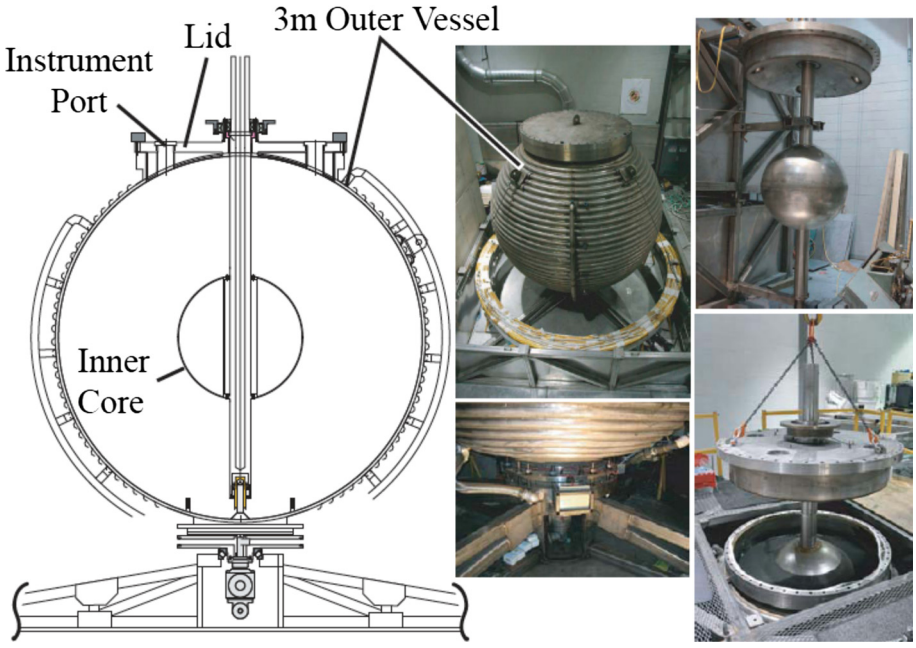

Fig. 3 Schematic and photos of the 3 m experiment. *Left*: a schematic of the experimental apparatus. *Photos, clockwise from top center*: the outer sphere; the inner sphere with shaft and lid; the inner sphere being lowered into the outer vessel, which is filled with water in this view; the bottom bearing and rotating fluid junction (allowing heating oil to be circulated in the jacket around the outer sphere)

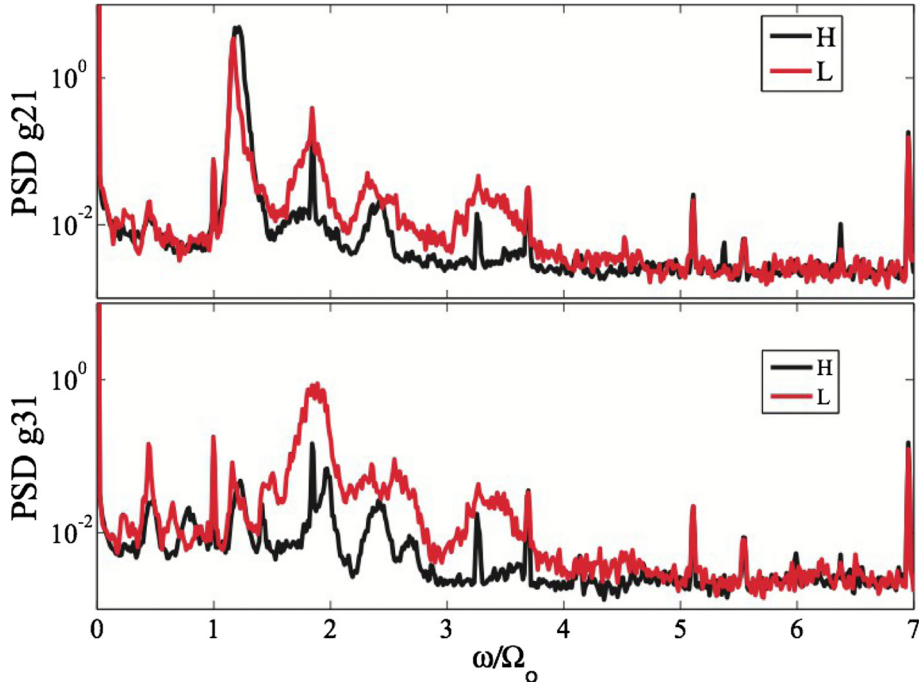

Fig. 4 Bistability in the 60 cm experiment. Induced magnetic field spectra from the 60 cm experiment at Ro = 2.7, $E = 3.2e-7$. *Top*: spectra (for both high and low torque states) of the Gauss coefficient with $l = 2$, $m = 1$. *Bottom*: the same for the coefficient with $l = 3$, $m = 1$. Note that much of the power in g21 is concentrated around a frequency of 1.18 Ω_o, corresponding to a velocity profile with $l = 3$, $m = 1$ and a frequency of 0.18 in the rotating frame, matching a wave seen in the 3 m device. The g31 coefficient is correlated with the low torque state. (From Zimmerman 2010)

analogous flows can be expected in their liquid cores. Precessional forcing has been proposed as an energy source for dynamos, including the geodynamo (Malkus 1968).

For the sodium experiments in 3 m to date, the device has been run at up to half speed on the outer sphere. At least 12 distinct non-dynamo states have been identified, with the states depending on Ro as in the case of the water experiments (as expected for non-magnetic states). The strength of the applied magnetic field can be varied in addition to varying Ro and Re. For the case of a self-sustaining dynamo, no applied field would be necessary (beyond some initial seed field, such as an ambient field or one due to random fluctuations). In addition, a power peak at a specific Ro has been identified. For the case of magnetized flow, a dipolar magnetic field is applied with a large electromagnet located around the experiment's equator.

Regarding the prospects for dynamo action in the 3 m device, a useful conceptual framework is the α-ω dynamo (Parker 1955). In this model, differential rotation converts poloidal field into (more intense) toroidal field (the ω effect), and then toroidal field is converted back into poloidal field via the so-called α effect, thus strengthening the original field and closing the dynamo feedback loop. During magnetized experiments in 3 m, the dipolar field applied by the external magnet provides a seed poloidal field. Any toroidal field present in the experiment is the result of the ω effect due to differential rotation in the fluid acting on the applied field. This toroidal field does not extend outside the experiment, however, and so can only be measured by a probe within the fluid volume. In order to have a diagnostic of the toroidal field, some measurements of magnetic field inside the flow have been taken at a single point using an inserted hall probe (in addition to the external field measurements made by an array of hall probes just outside the experiment). From these measurements, it is seen that the azimuthal field is significantly stronger than the local applied field, which has radial and vertical components. This is interpreted as a sign of the ω effect operating in the experiment, converting poloidal magnetic field (in this case the dipolar applied field) into toroidal (i.e., azimuthal) magnetic field. While the strong differential rotation of the flow for some Ro supplies significant ω effect, so far no states have been found with strong enough α effect to give self-sustaining dynamo action. Finally, looking at global magnetic field measurements, a dipole gain of up to 10 % has been observed in the experiment, though these states require an external applied field, and thus are not dynamo states (Zimmerman et al. 2014).

Simulations

Numerical simulations complement the observational and experimental work detailed above, providing flexibility in parameters as well as detailed information about the entire system. Motivated by observational and experimental results, simulations have shed light on various processes that may be at work in those systems and in turn motivate new experimental studies. Much work has been done in numerical studies relevant to the observations and experiments described above, including simulations of models of the geodynamo and direct numerical simulations of spherical Couette flow. This includes work on both hydrodynamic and hydromagnetic phenomena in spherical Couette, as well as studies of dynamo action in this and related geometries (see Wei et al. (2012) for a good overview, which we follow in the sections below, with updates). We first review hydrodynamic studies of spherical Couette flow, in which no magnetic field is present, before moving on to the magnetized case. Finally, we close this section with a discussion of some dynamo studies and their relevance for experiments.

Hydrodynamic studies

For the case of hydrodynamic spherical Couette flow, generally three limits can be distinguished (see Fig. 5): the case of outer stationary (the limit $|\mathrm{Ro}| \to \infty$) and the case of rapid outer rotation with either the inner sphere sub-rotating ($\mathrm{Ro} \to -0$) or with it super-rotating ($\mathrm{Ro} \to +0$). For the outer stationary case, a jet of fluid comes off the inner sphere, setting up a poloidal return flow (Fig. 5a). In the latter two cases, the bulk of the fluid spins with the outer sphere, while the volume of fluid inside the tangent cylinder spins under the influence of both the inner and outer spheres, and the velocity jump across the tangent cylinder is accomodated by a thin shear layer (Fig. 5b). This so-called Stewartson layer was first predicted by Stewartson (1966), who analytically studied the case of spherical Couette with strong overall rotation and infinitesimal differential rotation. For strong forcing, both the equatorial jet (infinite Ro) and the Stewartson layer ($|\mathrm{Ro}| \ll 1$) develop instabilities, which require numerical studies to elucidate.

Instabilities develop in the Stewartson layer of an overall rapidly rotating system when the differential rotation becomes sufficiently large. They were studied numerically in Hollerbach (2003) for a radius ratio of $r_i/r_o = 1/3$. In this study, the primary concern was the dependence of the instabilities on the sign of Ro. This work was partly motivated by a discrepancy in the experimental results obtained by Hide and Titman (1967) and Früh and Read (1999) regarding the effect of changing the sign of Ro; the original analysis of Busse (1968) had predicted that the system should be symmetric about $\mathrm{Ro} = 0$. Hollerbach (2003) found that $\mathrm{Ro} > 0$ (inner super-rotating) results in non-axisymmetric instabilities of the axisymmetric base state that have progressively larger azimuthal wavenumbers m for lower E (i.e., faster overall rotation). However,

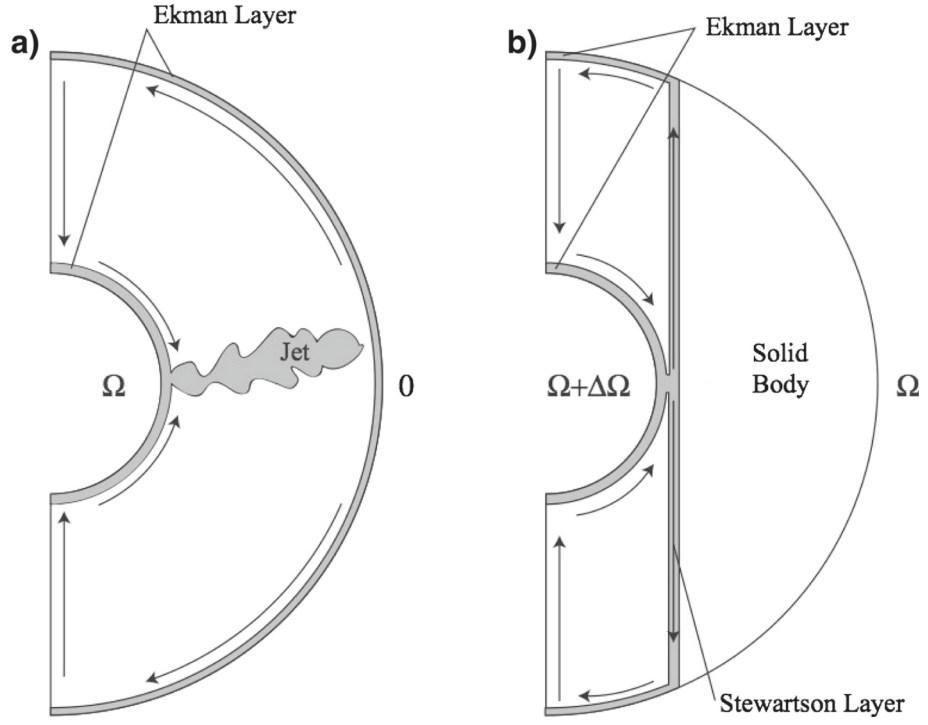

Fig. 5 General circulation patterns for spherical Couette flow. Flow patterns for the case of outer sphere stationary (**a**) and rapidly rotating (**b**). For **a**, the super-rotating inner sphere pumps fluid out into the bulk in the form of an equatorial jet, with a poloidal return flow. For **b**, the fluid outside the tangent cylinder spins in solid body with the outer sphere, while the fluid inside the tangent cylinder spins at a rate intermediate between the two spheres, with Ekman pumping along the boundaries of the tangent cylinder. The velocity jump across the boundary of the tangent cylinder is accommodated by the Stewartson layer, a region of high shear. (From Zimmerman 2010)

the instability has azimuthal wavenumber $m = 1$ for most of the range of E considered (down to 10^{-5}) for $\mathrm{Ro} < 0$ (inner sub-rotating). Thus, the sign of Ro for values near zero is significant, while the limits of infinite Ro are the same for both positive and negative values. In Hollerbach et al. (2004), stronger differential rotation was studied numerically and experimentally for the case $\mathrm{Ro} > 0$. They found that for sufficiently strong differential rotation a series of mode transitions back to smaller azimuthal wavenumbers occurs.

Another interesting regime is found near $\mathrm{Ro} = -2$, in which the spheres are counter-rotating, with the same angular frequencies. In this regime (with the relative sizes of the spheres also possibly playing a role), the bulk of the fluid is at rest in an inertial frame, and thus while the flow can be strongly driven, the influence of rotation is small (see, e.g., Guervilly and Cardin 2010).

Wicht (2014) performed an extensive study of wide-gap spherical Couette flow (with Earth-like radius ratio $r_i/r_o = 0.35$) across a wide range of parameter space. The study varied both outer sphere rotation (i.e., E) and the amount of differential rotation (i.e., Ro) over a wide range. Specifically, the study covered the following range of parameters: $10^2 \leq |\mathrm{Ro}/E| \leq 10^5$ and $10^4 \geq E \geq 10^{-6}$ (where the length scale used is $L = r_o - r_i$ in the definition of E). The results are consistent with previous numerical and experimental studies where the parameters overlap. For slow overall rotation, an equatorial jet formed that eventually developed instabilites as the inner sphere rotation rate (i.e., Ro) was increased and the Coriolis force did not have a significant effect on the flow. For fast overall rotation (i.e., low Ekman number), a Stewartson layer is formed and develops various instabilities as differential rotation is increased. In addition, inertial waves are found, which are possibly driven by instabilities in the Stewartson layer, as posited by Rieutord et al. (2012).

Hydromagnetic studies

For the case of hydromagnetic phenomena, a number of studies have addressed various aspects of magnetic spherical Couette flow. Starting with weak fields, the introduction of magnetic fields generally modifies the Stewartson layer (in the case of rapid overall rotation) or the equatorial jet (in the case of outer stationary or slow outer rotation); as the applied field gets stronger, it can eventually dominate rotational effects, with field lines structuring the flow. As in the non-magnetic case, the axisymmetric base state was studied analytically (in Starchenko 1998) as

well as numerically (Dormy et al. (1998, 2002), Hollerbach (2000), Hollerbach and Skinner (2001), and Hollerbach et al. (2007)). A discussion of a number of recent results can be found in Chp. 7 of Rüdiger et al. (2013) and in Wei et al. (2012). For the case of an applied field that is axisymmetric about the rotation axis of the spheres, the fluid is divided into regions magnetically coupled to either one or both of the spheres (see, e.g., Hollerbach and Skinner (2001)). As in the hydrodynamic case, jets and free shear layers can appear to accommodate the adjustment of the fluid rotation rate between these various regions.

For the case of strong overall rotation, the presence of a magnetic field can alter the Stewartson layer. In strong magnetic fields, free shear layers called Shercliff layers tend to form along magnetic field lines, and Ekman layers are modified by the magnetic field and called Hartmann layers (see, e.g., Rüdiger et al. 2013). Starchenko (1998) performed an asymptotic study of magnetic spherical Couette with an axial applied field, finding that a Shercliff layer formed at the tangent cylinder. He also considered a dipolar applied field, which when sufficiently strong results in two rigidly rotating regions, with the shear layer between them following the field lines that are tangent to the outer sphere at its equator. Here, both spheres were insulating.

In the case of conducting spheres, a similar setup can result in super-rotation. Starchenko (1997) and Dormy et al. (1998, 2002) numerically found a super-rotating jet (the fluid rotates faster than the inner sphere) in the case of a stationary outer sphere with a conducting inner boundary and an imposed dipolar field, while insulating boundaries gave results consistent with previous asymptotic findings. Hollerbach (2001) studied how varying the imposed field geometry and the boundary conditions (insulating or conducting) could give rise to super- or counter-rotating jets.

Hollerbach and Skinner (2001) found that for the case of a stationary outer sphere and a strong axial field that stronger magnetic field stabilizes flow: the shear layer goes unstable to non-axisymmetric disturbances at higher and higher Re. Wei and Hollerbach (2008) also considered spherical Couette flow with outer stationary and with overall rotation, with or without an axial magnetic field, and studied the stability of Stewartson (without an applied field, but with overall rotation) and Shercliff (with an applied field) layers. They found that the instabilities of the Shercliff layer were symmetric about the solid body case (that is, inner sphere sub- and super-rotation behaved in the same way), while as noted above the Stewartson layer instabilities are asymmetric about this case. By considering the mixed case (overall rotation with an applied field), they showed that these two different cases are smoothly connected. For a useful overview of this work, see also Wei et al. (2012).

Gissinger et al. (2011) investigated instabilities of magnetized spherical Couette flow for a variety of Ro, imposed fields, and magnetic boundary conditions. They found that an applied field can suppress hydrodynamic instabilities of the Stewartson layer or equatorial jet, but can also introduce new instabilities, associated either with disruption of the axisymmetry of the meridional return flow or with the Shercliff layer going unstable to non-axisymmetric modes. Figueroa et al. (2013) studied spherical Couette flow in a dipolar field (motivated by the DTS experiment), finding that fluctuations in the magnetic field had most of their energy located near the inner sphere (where the dipolar field is strongest) but are due to velocity fluctuations that originate in the outer boundary layer. These velocity fluctuations originate in two coupled instabilities: a high-latitude Bödewadt-type boundary layer instability and a secondary non-axisymmetric instability of a centripetal jet near the equator of the outer sphere. Generally, the introduction of magnetic fields provides new ways to both stabilize and destabilize the equatorial jets and Stewartson layers found in the non-magnetic case. In addition, applied magnetic fields can lead to the formation of flow structures with no analog in the hydrodynamic case, and these structures can in turn develop their own instabilities.

Dynamo studies

There have also been numerical investigations of dynamo action in spherical Couette flow. One type of simulation is the kinematic dynamo, which ignores the back reaction of the magnetic field on the flow. In these simulations, the flow of a conducting fluid in spherical Couette is calculated first. Then, this flow pattern is used in the magnetic induction equation to determine if there are any growing magnetic fields, which is a sign of dynamo action.

In the kinematic dynamo, a larger aspect ratio (r_o/r_i) and conducting boundary layers favor dynamo action (Wei et al. 2012). The similar case of the kinematic dynamo in a full-sphere (i.e., no inner sphere), but with boundary conditions that mimic the tangent cylinder flow of spherical Couette (polar caps that rotate at a different rate from the rest of the spherical boundary), was studied by Schaeffer and Cardin (2006). Using a quasi-geostrophic model allowed them to reach very low Ekman number $\left(10^{-8}\right)$, and they considered the case of low Pm (resulting in a scale separation between the magnetic and velocity fields, and making the results relevant to liquid metal experiments and planetary cores). The kinematic dynamo found was interpreted as an α-ω type, with differential rotation providing the ω effect and Rossby waves (which are instabilities of the internal shear layer) providing the α effect.

In addition to kinematic dynamos, non-linear dynamos have also been studied, in which the back reaction of the

magnetic field generated by dynamo action onto the fluid flow is included (Guervilly and Cardin 2010). Guervilly and Cardin (2010) found that dynamo action was achieved in spherical Couette flow when non-axisymmetric hydrodynamical instabilities were excited and Rm was sufficiently high. For the case of outer stationary, the critical Rm was of the order of a few thousands, with its value increasing with increasing Re. Specifically, the critical value of Pm was found to be 1. With outer rotation, the critical Pm was reduced by a factor of two (indicating overall rotation is more favorable for dynamo action), and for intermediate values of rotation $\left(E = 10^{-3}\right)$, a favorable window for dynamo action was found, with a critical Rm of 300. The authors speculate that this may be due to an enhanced shear layer around the inner core, which however becomes unstable at lower E, eliminating this favorable regime for faster rotation. They also looked at the effect of ferromagnetic boundary conditions, finding minimal impact on the dynamo threshold though the strength of the saturated magnetic field above the dynamo threshold was enhanced in the ferromagnetic regions. These studies can offer hints regarding what setups may favor dynamo action, including that inner conducting boundaries and large aspect ratios may be more favorable to dynamo action (Wei et al. 2012).

The phenomenon of intermittency near the onset of dynamo action has been investigated numerically by Raynaud and Dormy (2013). They found intermittency in the magnetic field near the dynamo threshold for a variety of boundary conditions (both spheres insulating, inner sphere conducting, and both ferromagnetic), with the intermittency eventually going away when the system is sufficiently above the dynamo threshold. This work may offer some guidance in the analysis of states observed in 3 m with bursts of magnetic field enhancement.

Finally, a comparison of smooth and rough inner boundaries for kinematic spherical Couette dynamos was made by Finke and Tilgner (2012). They considered the case of outer stationary, with $r_i/r_o = 1/3$, and compared the case of flow driven by a smooth inner sphere with no-slip boundary conditions and the case of flow driven by a volume force near the inner sphere (to simulate a rough inner sphere surface). The case of a rough inner sphere results in a reduction of the critical inner rotation rate for dynamo action by a factor of 10. This case also results in a thicker boundary layer and equatorial jet, which also make dynamo action somewhat more favorable. This work is of particular interest in future plans for roughening the inner sphere of 3 m via the attachment of baffles, thus increasing the coupling of the inner sphere with the bulk fluid and increasing the strength of the equatorial jet off the inner sphere and associated poloidal flows.

Open questions and future directions

In the above surveys of experimental and numerical results for magnetic spherical Couette and related flows, a number of recurring themes can be seen. These include the effects of turbulence on dynamo action, including the value of the critical Rm for a flow, and the effect of boundary conditions, whether insulating, conducting, or ferromagnetic. For spherical Couette flow in particular, overall system rotation also often has a marked effect on the dynamics of the system as compared to the case of a stationary outer sphere. A major open question is how to achieve dynamo action in a laboratory spherical Couette system. Numerical simulations have found dynamo action in spherical Couette systems, so an experimental spherical Couette dynamo should also be possible. However, experimental complications mean this is still a challenging endeavor. In particular, in simulations, the critical Rm to achieve dynamo action is generally on the order of hundreds to thousands, leading one to expect a similar value will be necessary in experiments. For hydromagnetic experiments, however, liquid metals are one of the few types of working fluid available (plasmas can also work but have their own complications) and have very small Pm, on the order of 10^{-5}. Since, Rm = RePm, this means that in order to reach the critical Rm for the spherical Couette system, experiments will have to have very large Re and will thus be turbulent. This turbulence in turn makes it very challenging to realistically simulate the experiments. Thus, the effect of turbulence on the dynamo threshold, and on the character of the dynamo itself, remains an open question.

The role of turbulence

Turbulence has generally been seen as making dynamo action more difficult. Certainly, it makes predicting the onset of dynamo action challenging. While kinematic dynamos have been found in spherical Couette flows (see, e.g., Wei et al. 2012), so far no dynamos have been found in the analogous, turbulent experiments. A turbulent velocity field will tend to tangle up any magnetic field lines that are present. If the correlations between the velocity fluctuations and those of the magnetic field have the right form, they can add coherently and result in an α effect. The tangling of the field lines can also result in an increase or decrease of dissipation of the magnetic field, resulting in an increase or decrease of the effective resistivity of the fluid (termed the β effect) (Steenbeck et al. 1966; Krause and Rädler 1980). An experimental observation of the β effect was first reported in Reighard and Brown (2001), with the turbulence leading to an increase in the effective resistivity of the fluid. As noted above, both positive and negative β effects have been seen in some of the experiments described above (Cabanes et al. 2014a; Nornberg et al. 2006). The influence of turbulence

is thus variable. In the two previous laboratory dynamos based on kinematic dynamos, the use of pipes to enforce an overall flow geometry also limited the effects of turbulent fluctuations (and the onset matched kinematic predictions, confirming the relative unimportance of turbulence for these systems). On the other hand, the VKS dynamo is fully turbulent, demonstrating that laboratory dynamos in an open geometry with turbulence are achievable. The VKS experiment brings up another question, namely the role of ferromagnetic boundary conditions in its dynamo mechanism, and the prospects for ferromagnetic boundaries in other experiments, to which we now turn.

The influence of boundaries

As shown by numerical simulations like those of Hollerbach (2001), the boundary conditions of spherical Couette flow (insulating or conducting) can have a dramatic effect on the flow dynamics. Bullard and Gubbins (1977) first investigated the effect of electromagnetic boundary conditions on dynamo action in a sphere, finding that an insulating boundary tended to suppress dynamo action due to the formation of a current sheet that inhibited regeneration of the magnetic field. In the case of ferromagnetic boundary conditions, numerical results have not shown a dramatic effect on the dynamo threshold in spherical Couette (though conducting vs. insulating can significantly affect the value of the critical Rm (Guervilly and Cardin 2010)). For the VKS experiment, dynamo action is only achieved when at least one of the impellers driving the flow is ferromagnetic. For experiments in a spherical geometry, as noted above, the MDE experiment did not achieve dynamo action with ferromagnetic impellers. For spherical Couette experiments, the 60 cm sodium experiment had a soft iron inner sphere installed for some experiments, which tended to result in more broadband fluctuations but did not result in a dynamo in the parameter range studied (Kelley 2009). The exact role played by the soft-iron impellers in the VKS dynamo remains unclear. Speaking generically, ferromagnetic material in a dynamo experiment has two main effects (see, e.g., Kelley (2009) for a discussion of the effect of ferromagnetic boundaries). First, it tends to locally concentrate magnetic field near it, since this minimizes the energy of the system. Second, magnetic fields leaving it to enter a lower permeability material (such as liquid sodium) lie approximately perpendicular to its surface. Thus, ferromagnetic material can change the local shape of magnetic fields, as well as changing the distribution of magnetic energy. Either or both mechanisms could be significant in the VKS dynamo. Gissinger et al. (2008) found using a numerical model of VKS that both ferromagnetic disks and ferromagnetic blades decreased the threshold for dynamo action.

Gissinger (2009) presented results of numerical simulations of VKS using a kinematic code, which by taking into account both the axisymmetric mean of the flow and its non-axisymmetric components could generate either an axial dipole or axial quadrupole. The competition between these two modes could then result in reversals of the dipole field when the symmetry of the system was broken (by having the two impellers counter-rotate at different rates). This model thus reproduced the axial dipole found in the experiment, including the stationary field in the case of impellers counter-rotating at the same frequency and an oscillating field with reversals in the case of different rotation frequencies. In order to investigate the role of the ferromagnetic discs, Nore et al. (2015) put forth a tentative model of dynamo action in VKS. According to this model, dynamo action in VKS is the result of a three-step process. First, toroidal energy accumulates in the disks (due to their large permeability); second, poloidal field is produced in the blade region of the impellers due to the interaction of recirculating fluid flow in between the blades with the toroidal field that accumulates in the disks; and finally, the bulk flow transports this poloidal field throughout the vessel, where the ω effect can then create toroidal field (which in turn accumulates in the disks, thus closing the loop). Thus, the ferromagnetic impellers are critical for supplying a localized α effect to enable the dynamo. The authors also note that this model shares similarities with the flux transport dynamo mechanism proposed for the solar dynamo, in that the conversion of poloidal to toroidal field occurs in a different location from the conversion of toroidal to poloidal field, thus requiring the intermediate transport of flux for the dynamo to operate. This could help to explain why MDE did not achieve a dynamo using VKS-type soft-iron impellers. If the dynamo were purely the result of local dynamo action at the site of the impellers, one would expect MDE to achieve a dynamo as well. If however the global transport of field is also an integral part of the dynamo mechanism, then differences in the flow patterns resulting from the different vessel geometries may help to explain the different outcomes with respect to dynamo action. Further investigation is needed to sort out these issues.

System rotation and helicity

As has been noted, the α-ω dynamo mechanism, and the decomposition of the magnetic and velocity fields into poloidal and toroidal components, provides a useful conceptual framework for laboratory dynamos. As far as the experimental challenge of achieving a dynamo in an Earth-like geometry is concerned, in spherical Couette flow, strong differential rotation means it is relatively easy to obtain a large ω effect (as seen in MDE, 3 m and DTS), but so far a strong α effect (necessary to close the feedback

loop) has proved more elusive. In the Riga and Karlsruhe dynamos, the α effect was achieved by organizing the overall flow pattern in pipes. In the VKS experiment, the only dynamo to date in an open geometry, the α effect seems to be present near the ferromagnetic impellers, possibly due to turbulent eddies coming off the impeller vanes. However, since dynamo action is only achieved with impellers that are ferromagnetic, which allows the build-up of strong toriodal fields within the impellers, it appears that these provide a necessary seed for the α effect to be sufficiently strong for dynamo action. In this view, for the case of non-ferromagnetic impellers, while the velocity fluctuations that could result in the α effect are still present, the toroidal field present is much weaker, and thus the poloidal field generated by the α effect near the impeller vanes is no longer sufficient for dynamo action.

In addition to differential rotation, spherical Couette systems can also have overall system rotation, which as noted above gives rise to three natural limit cases ($\mathrm{Ro} \to \infty$, $\mathrm{Ro} \to +0$, and $\mathrm{Ro} \to -0$). Also, while the MDE experiment does not rotate overall, its double-vortex flow (via the two counter-rotating impellers) does make use of large-scale rotation in the flow, with the strong toroidal flows set up in it sharing similarities with those set up by differential rotation in spherical Couette devices (though of course with the important difference of being equatorially anti-symmetric, while those in spherical Couette devices are symmetric). A natural way of viewing this setup is in terms of helicity. Helical flows, which have both a net rotation and flow along the axis of rotation, provide a natural source for the α effect (see, e.g., Parker 1955), and thus while pure differential rotation only provides an ω effect in the flow, rotation is also often a key ingredient of the α effect generally needed to close the dynamo loop. Looking to astrophysical bodies, the often close alignment found between the direction of dipolar fields and the axis of rotation, such as is found for the Earth, also hints at rotational effects being important in organizing the geometry of the magnetic field that results, if not in the initial generation of this field (see, e.g., Chp. 2 of Rüdiger and Hollerbach 2004). While the presence of helicity can result in the α effect, the exact requirements are less clear. Livermore et al. (2007) found that while local helicity can participate in kinematic dynamos in spherical shells, the flows most favorable for dynamo action had zero net helicity. This is of interest because the inertial waves found in rapidly rotating devices like 60 cm (e.g., Kelley 2009) and 3 m (e.g., Zimmerman 2010) have zero net helicity but patches of strong helicity (Zimmerman 2010). Inertial waves have been proposed as a possible source of dynamo action (Moffatt 1970). Being Coriolis-restored wave modes, inertial modes require rapid rotation, and interestingly can contain a large amount of power even in highly turbulent flows, possibly providing a robust mechanism for dynamo action even in the presence of large turbulent fluctuations.

Experimental improvements

Considering the prospects for liquid sodium experiments, it appears that an increase in power may be needed in order to reach the critical Rm for spherical Couette flow. Alternatively, modifications to enhance the conversion of toroidal flow into poloidal flow (perhaps by enhancing the equatorial jet and associated meridional return flow by roughening the inner sphere) could improve the prospects for dynamo action. In addition, for the purposes of understanding the dynamics of magnetized spherical Couette flow, and any future associated dynamo action, improved flow velocimetry would be beneficial. In the VKS experiment, dynamo action has been achieved but is still not well understood partly due to the difficulty in determining the exact behavior of the turbulent fluid flow near the impellers. In spherical Couette flow with smooth boundaries, this is not as difficult, but flow velocimetry remains challenging. Ultrasound can be used, as in DTS, or an analogous water experiment can be constructed (as was done for MDE) to allow more conventional methods to be used for velocity measurements. Another exciting prospect is the possibility of using modal acoustic velocimetry to measure azimuthal velocity profiles in rotating sodium experiments (Triana et al. 2014).

Related experiments

In addition to the ongoing liquid metal spherical Couette experiments detailed above, a number of related experiments can also provide insights into dynamo action in an Earth-like geometry. The Princeton MRI experiment (Ji et al. 2006; Nornberg et al. 2010; Roach et al. 2012) is a Taylor-Couette liquid metal gallium experiment. With similar driving in a different geometry (shear between inner and outer cylindrical boundaries), its results can be useful for comparison with spherical Couette devices. The Madison Plasma Dynamo Experiment (Collins et al. 2012; Katz et al. 2012) has a whole-sphere geometry and uses plasma as the conducting medium. This allows it to access a different range in Re-Rm space, since the plasma's Pm differs significantly from that of liquid metals. Moreover, the value of Pm is adjustable, opening up the possibility for new experimental investigations of the Pm dependence of flow dynamics. Also, the flow is driven from the outer boundary, with the experiment able to impose an arbitrary velocity profile at that location. Upcoming results from this experiment promise to be very interesting and should shed light on the prospects for dynamo action in a spherical geometry.

Conclusions

While much progress has been made in understanding both spherical Couette flow and dynamo action in this geometry, as well as dynamo action in planetary cores, there are still many open questions. A potential synthesis of numerical work with experimental and observational studies could be found in the transformation of geomagnetism into a predictive science. The Earth's core is characterized by some extreme parameters, and governed by non-linear partial differential equations, some of which have parameters that are not tightly constrained. Another similarly complex, non-linear system is the Earth's atmosphere, which nonetheless has proven amenable to prediction. Weather prediction is now a fairly refined and robust system, though the chaotic nature of the atmosphere limits the timespan over which predictions can usefully be made. A technique that has had great success in weather prediction is data assimilation, whereby estimates of the state of the Earth's atmosphere are improved by incorporating atmospheric measurements as they come in to determine which of a number of states being evolved forward is most compatible with the new data. Thus, this technique provides a straightforward way of using the history of the system to better estimate parameters of it that have not been directly observed, in turn allowing better prediction of its future evolution. Several groups have used these techniques to better understand and forecast the geodynamo (Fournier et al. 2010; Tangborn and Kuang 2015). It is likely that combining simulation studies, data assimilation, and experimental hydromagnetic data could yield new insights on turbulent dynamos.

Abbreviations

DTS: Derviche Tourneur Sodium (an experiment in Grenoble, France); EMF: electromotive force; LDV: laser Doppler velocimetry (a technique for measuring velocities in transparent fluids); MDE: Madison dynamo experiment (an experiment at the University of Wisconsin-Madison); UDV: ultrasound Doppler velocimetry (a technique for measuring velocities, can be used in liquid sodium); VKS: von Kármán sodium (an experiment in Cadarache, France)

Competing interests

The authors declare that they have no competing interests.

Authors' contributions

MMA drafted the paper and with DSZ took the data presented in Fig. 4. DSZ performed the analysis of this data. DPL and DRS collaborated with MMA in revising the manuscript, and DPL and DSZ made the figures. All authors read and approved the final manuscript.

Authors' information

DPL is a professor of physics and geology at the University of Maryland, College Park. DRS is currently a post-doc under DPL, and MMA is a PhD student under DPL. DSZ was formerly a PhD student and then post-doc under DPL.

Acknowledgements

The authors are grateful to Santiago Triana and Henri-Claude Nataf for previous collaboration and discussions. They also would like to thank Daniel Serrano for help with editing the manuscript and Laurent Hindryckx for the initial image used in preparing Fig. 2. The authors gratefully acknowledge the support of the NSF via grant EAR-1417148. Finally, they thank the two anonymous reviewers whose comments helped to substantially improve this work.

Author details

[1]Institute for Research in Electronics and Applied Physics, University of Maryland, College Park, 20742 MD, USA. [2]Department of Physics, University of Maryland, College Park, MD, USA. [3]Department of Geology, University of Maryland, College Park, MD, USA. [4]Pliant Energy Systems, Brooklyn, NY, USA.

Received: 13 January 2015 Accepted: 31 August 2015
Published online: 17 September 2015

References

Acuña M, Connerney J, Ness N, Lin R, Mitchell D, Carlson C, McFadden J, Anderson K, Rème H, Mazelle C, Vignes D, Wasilewski P, Cloutier P (1999) Global distribution of crustal magnetization discovered by the Mars Global Surveyor MAG/ER experiment. Science 284:790–793

Berhanu M, Monchaux R, Fauve S, Mordant N, Pétrélis F, Chiffaudel A, Daviaud F, Dubrulle B, Marié L, Ravelet F, Bourgoin M, Odier P, Pinton J-F, Volk R (2007) Magnetic field reversals in an experimental turbulent dynamo. EPL 77(5):59001

Brito D, Alboussière T, Cardin P, Gagnière N, Jault D, La Rizza P, Masson J-P, Nataf H-C, Schmitt D (2011) Zonal shear and super-rotation in a magnetized spherical Couette-flow experiment. Phys Rev E 83:066310

Bullard E, Gellman H (1954) Homogeneous dynamos and terrestrial magnetism. Philos T R Soc S-A 247(928):213–278

Bullard E, Gubbins D (1977) Generation of magnetic fields by fluid motions of global scale. Geophys Astro Fluid 8:43–56

Busse F (1968) Shear flow instabilities in rotating systems. J Fluid Mech 33:577–589

Cabanes S, Schaeffer N, Nataf H-C (2014) Magnetic induction and diffusion mechanisms in a liquid sodium spherical Couette experiment. Phys Rev E 90:043018

Cabanes, S, Schaeffer N, Nataf H-C (2014a) Turbulence reduces magnetic diffusivity in a liquid sodium experiment. Phys Rev Lett 113:184501

Cardin P, Brito D, Jault D, Nataf H-C, Masson J-P (2002) Towards a rapidly rotating liquid sodium dynamo experiment. Magnetohydrodynamics 38:177–189

Collins C, Katz N, Wallace J, Jara-Almonte J, Reese I, Zweibel E, Forest C (2012) Stirring unmagnetized plasma. Phys Rev Lett 101:115001

Cowling T (1934) The stability of gaseous stars. Mon Not R Astron Soc 94:768–782

Dormy E, Cardin P, Jault D (1998) MHD flow in a slightly differentially rotating spherical shell, with conducting inner core, in a dipolar magnetic field. Earth Planet Sc Lett 160:15–30

Dormy E, Jault D, Soward A (2002) A super-rotating shear layer in magnetohydrodynamic spherical Couette flow. J Fluid Mech 452:263–291

Dudley M, James R (1989) Time-dependent kinematic dynamos with stationary flows. Proc R Soc Lon Ser-A 425:407

Eddy J (1978) Historical and arboreal evidence for a changing sun. In: Eddy J (ed). The New Solar Physics. Westview Press, Coulder, Co.

Figueroa A, Schaeffer N, Nataf H-C, Schmitt D (2013) Modes and instabilities in magnetized spherical Couette flow. J Fluid Mech 716:445–469

Finke K, Tilgner A (2012) Simulations of the kinematic dynamo onset of spherical Couette flows with smooth and rough boundaries. Phys Rev E 86:016310

Fournier A, Hulot G, Jault D, Kuang W, Tangborn A, Gillet N, Canet E, Aubert J, Lhuillier F (2010) An introduction to data assimilation and predictability in geomagnetism. Space Sci Rev 155:247–291

Früh W, Read P (1999) Experiments on a barotropic rotating shear layer. Part 1. Instability and steady vortices. J Fluid Mech 383:143–173

Gailitis A, Lielausis O, Dement'ev S, Platacis E, Cifersons A, Gerbeth G, Gundrum T, Stefani F, Christen M, Hänel H, Will G (2000) Detection of a flow induced magnetic field eigenmode in the riga dynamo facility. Phys Rev Lett 84(19):4365–4368

Gailitis A, Lielausis O, Platacis E, Dement'ev S, Cifersons A, Gerbeth G, Gundrum T, Stefani F, Christen M, Will G (2001) Magnetic field saturation in the riga dynamo experiment. Phys Rev Lett 86(14):3024–3027

Gailitis A, Gerbeth G, Gundrum T, Lielausis O, Platacis E, Stefani F (2008) History and results of the riga dynamo experiments. C R Phys 9:721–728

Gauss C (1839) Allgemeine theorie des erdmagnetismus. In: Resultate aus Den Beobachtungen Magnetischen Vereins Im Jahre 1838. pp 1–57

Garrick-Bethel I, Weiss B, Shuster D, Buz J (2009) Early lunar magnetism. Science 323:356–359

Gissinger C, Iskakov A, Fauve S, Dormy E (2008) Effect of magnetic boundary conditions on the dynamo threshold of von Kármán swirling flows. Europhys Lett 82:29001
Gissinger C (2009) A numerical model of the VKS experiment. Europhys Lett 87:39002
Gissinger C, Ji H, Goodman J (2011) Instabilities in magnetized spherical Couette flow. Phys Rev E 84:026308
Glatzmaier G, Roberts P (1995) A three-dimensional self-consistent computer simulation of a geomagnetic field reversal. Nature 377:203–209
Guervilly C, Cardin P (2010) Numerical simulations of dynamos generated in spherical Couette flows. Geophys Astro Fluid 104:221–248
Hide R, Titman C (1967) Detached shear layers in a rotating fluid. J Fluid Mech 29:39–60
Hollerbach R (2000) Magnetohydrodynamic flows in spherical shells. In: Egbers C, Pfister G (eds). Physics of rotating fluids (Lecture notes in physics), 1st. Springer, Heidelberg
Hollerbach, R (2001) Super- and counter-rotating jets and vortices in strongly magnetic spherical Couette flow. In: Chossat P, Armbruster D, Oprea J (eds). Dynamo and dynamics: a mathematical challenge. Kluwer, Dordrecht, the Netherlands
Hollerbach R, Skinner S (2001) Instabilities of magnetically induced shear layers and jets. Proc R Soc A 457:785–802
Hollerbach R (2003) Instabilities of the Stewartson layer part 1. The dependence on the sign of Ro. J Fluid Mech 492:289–302
Hollerbach R, Futterer B, More T, Egbers C (2004) Instabilities of the Stewartson layer: part 2. Supercritical mode transitions. Theor Comp Fluid Dyn 18:197–204
Hollerbach R, Canet E, Fournier A (2007) Spherical Couette flow in a dipolar magnetic field. Eur J Mech B-Fluid 26:729–737
Jackson A, Jonkers A, Walker M (2000) Four centuries of geomagnetic secular variation from historical records. Philos T Roy Soc A 358:957–990
Ji H, Burin M, Schartman E, Goodman J (2006) Hydrodynamic turbulence cannot transport angular momentum effectively in astrophysical disks. Nature 444:343–346
Kaplan E, Clark M, Nornberg M, Rahbarnia K, Rasmus A, Taylor N, Forest C, Spence E (2011) Reducing global turbulent resistivity by eliminating large eddies in a spherical liquid-sodium experiment. Phys Rev Lett 106:254502
Katz N, Collins C, Wallace J, Clark M, Weisberg D, Jara-Almonte J, Reese I, Wahl C, Forest C (2012) Magnetic bucket for rotating unmagnetized plasma. Rev Sci Instrum 83:063502
Kelley D, Triana S, Zimmerman D, Brawn B, Lathrop D, Martin D (2006) Driven inertial waves in spherical Couette flow. Chaos 16:1105
Kelley D, Triana S, Zimmerman D, Tilgner A, Lathrop D (2007) Inertial waves driven by differential rotation in a planetary geometry. Geophys Astro Fluid 101(5-6):469–487
Kelley D (2009) Rotating, hydromagnetic laboratory experiment modelling planetary cores. PhD thesis, University of Maryland, Bethesda, MD, USA
Kelley D, Triana S, Zimmerman D, Lathrop D (2010) Selection of inertial modes in spherical Couette flow. Phys Rev E 81:026311
Kivelson M, Khurana K, Russel C, Walker R, Warnecke J, Coroniti F, Polanskey C, Southwood D, Schubert G (1996) Discovery of Ganymede's magnetic field by the Galileo spacecraft. Nature 384:537–541
Krause K, Rädler K (1980) Mean-field magnetohydrodynamics and dynamo theory. Pergamon Press, New York
Langel R (1993) The use of low altitude satellite data bases for modelling of core and crustal fields and the separation of external and internal fields. Surv Geophys 14:31–87
Larmor J (1919) How could a rotating body such as the sun become a magnet? Rep Brit Assoc Adv Sci A 87:159–160
Livermore P, Hughes D, Tobias S (2007) The role of helicity and stretching in forced kinematic dynamos in a spherical shell. Phys Fluids 19:057101
Malkus W (1968) Precession of the earth as the cause of geomagnetism. Science 160:259–264
Merrill R, McElhinny M, McFadden P (1996) The magnetic field of the Earth: paleomagnetisim, the core, and the deep mantle. Academic Press, San Diego
Moffatt H (1970) Dynamo action associated with random inertial waves in a rotating conducting fluid. J Fluid Mech 44:705–719
Monchaux R, Berhanu M, Bourgoin M, Moulin M, Odier P, Pinton J-F, Volk R, Fauve S, Mordant N, Pétrélis F, Chiffaudel A, Daviaud F, Dubrulle B, Gasquet C, Marié L, Ravelet F (2007) Generation of a magnetic field by dynamo action in a turbulent flow of liquid sodium. Phys Rev Lett 98(4): 044502–4
Nataf H-C, Alboussière T, Brito D, Cardin P, Gagnière N, Jault D, Masson J-P, Schmitt D (2006) Experimental study of super-rotation in a magnetostrophic spherical Couette flow. Geophys Astro Fluid 100:281–298
Nataf H-C, Alboussière T, Brito D, Cardin P, Gagnière N, Jault D, Schmitt D (2008) Rapidly rotating spherical Couette flow in a dipolar magnetic field: an experimental study of the mean axisymmetric flow. Phys Earth Planet In 170:60–72
Nornberg M, Forest C, Plihon N (2014a) Soft-iron impellers in the Madison Sodium Dynamo Experiment. New Orleans, LA Note: this was a presentation at the APS DPP meeting Available at the following website: http://plasma.physics.wisc.edu/uploadedfiles/talk/APS-DPP2014Nornberg1029.pdf
Nornberg M, Spence E, Kendrick R, Jacobson C, Forest C (2006) Measurements of the magnetic field induced by a turbulent flow of liquid metal. Phys Plasmas 13:055901
Nornberg M, Spence E, Kendrick R, Jacobson C, Forest C (2006a) Intermittent magnetic field excitation by a turbulent flow of liquid sodium. Phys Rev Lett 97:044503
Nornberg M, Ji H, Schartman E, Roach A, Goodman J (2010) Observation of magnetocoriolis waves in a liquid metal Taylor-Couette experiment. Phys Rev Lett 104(7):074501
Nornberg M, Taylor N, Forest C, Rahbarnia K, Kaplan E (2014) Optimization of magnetic amplification by flow constraints in turbulent liquid sodium. Phys Plasmas 21:055903
Nore C, Léorat J, Guermond J-L, Giesecke A (2015) Mean-field model of the von Kármán sodium dynamo experiment using soft iron impellers. Phys Rev E 91:013008
Olson P (2013) Experimental dynamos and the dynamics of planetary cores. Annu Rev Earth Pl Sc 41:153–81
Parker E (1955) Hydromagnetic dynamo models. Astrophys J 122:293–314
Ponomarenko Y (1973) Theory of the hydromagnetic generator. J Appl Mech Tech Phy 14:775–778
Raynaud R, Dormy E (2013) Intermittency in spherical Couette dynamos. Phys Rev E 87:033011
Reighard A, Brown M (2001) Turbulent conductivity measurements in a spherical liquid sodium flow. Phys Rev Lett 86(13):2794–2797
Rieutord M, Triana S, Zimmerman D, Lathrop D (2012) Excitation of inertial modes in an experimental spherical Couette flow. Phys Rev E 86:026304
Roach A, Spence E, Gissinger C, Edlund E, Sloboda P, Goodman J, Ji H (2012) Observation of a free-Shercliff-layer instability in cylindrical geometry. Phys Rev Lett 108:154502
Roberts G (1972) Dynamo action of fluid motions with two-dimensional periodicity. Philos T R Soc S-A 271:411
Rüdiger G, Hollerbach R (2004) The magnetic universe. Wiley-VCH, Weinheim
Rüdiger G, Kitchatinov L, Hollerbach R (2013) Magnetic processes in astrophysics: theory, simulations, experiments. Wiley-VCH, Weinheim
Sams B, Golub L, Weiss N (1992) X-ray observations of sunspot penumbral structure. Astrophys J 399:313–317
Schaeffer N, Cardin P (2006) Quasi-geostrophic kinematic dynamos at low magnetic Prandtl number. Earth Planet Sc Lett 245:595–604
Schmitt D, Cardin P, La Rizza P, Nataf H-C (2013) Magneto-coriolis waves in a spherical Couette flow experiment. Eur J Mech B-Fluid 37:10–22
Shew W, Lathrop D (2005) Liquid sodium model of geophysical core convection. Phys Earth Planet In 153:136–149
Sisan D (2004) Hydromagnetic turbulent instability in liquid sodium experiments. PhD thesis, University of Maryland, College Park, MD, USA
Sisan D, Mujica N, Tillotson W, Huang Y, Dorland W, Hassam A, Antonsen T, Lathrop D (2004) Experimental observation and characterization of the magnetorotational instability. Physical Review Letters 93(11):114502
Spence E, Nornberg M, Jacobson C, Kendrick R, Forest C (2006) Observation of turbulence-induced large scale magnetic field. Phys Rev Lett 96:055002
Spence E, Nornberg M, Jacobson C, Parada C, Taylor N, Kendrick R, Forest C (2007) Turbulent diamagnetism in flowing liquid sodium. Phys Rev Lett 98:164503
Starchenko S (1997) Magnetohydrodynamics of a viscous spherical shear layer rotating in a strong potential field. J Exp Theor Phys 85:1125
Starchenko, S (1998) Magnetohydrodynamic flow between insulating shells rotating in strong potential field. Phys Fluids 10:2412–2420

Steenbeck M, Kirko I, Gailitis A, Klyavinya A, Krause F, Laumanis I, Lielausis O (1968) Experimental discovery of the electromotive force along the external magnetic field induced by a flow of liquid metal (α-effect). Sov Phys Dokl 13:443
Steenbeck M, Krause F, Rädler K (1966) Berechnung der mittleren Lorentz-Feldstärke für ein elektrisch leitendes medium in turbulenter, durch Coriolis-Kräfte beeinfluß bewegung. Z Naturforsch 21a:369
Stewartson K (1966) On almost rigid rotations 2. J Fluid Mech 26:131–144
Stieglitz R, Müller U (2001) Experimental demonstration of a homogeneous two-scale dynamo. Phys Fluids 13:561–564
Takahashi F, Matsushima M, Honkura Y (2005) Simulations of a quasi-Taylor state geomagnetic field including polarity reversals on the earth simulator. Science 309:459–461
Tangborn A, Kuang W (2015) Geodynamo model and error parameter estimation using geomagnetic data assimilation. Geophys J Int 200:664–675
Triana S, Zimmerman D, Lathrop D (2012) Precessional states in a laboratory model of the Earth's core. J Geophys Res 117:B04103
Triana S, Zimmerman D, Nataf H-C, Thorette A, Lekic V, Lathrop D (2014) Helioseismology in a bottle: modal acoustic velocimetry. New J Phys 16:113005
Wei X, Hollerbach R (2008) Instabilities of Shercliff and Stewartson layers in spherical Couette flow. Phys Rev E 78:026309
Wei X, Jackson A, Hollerbach R (2012) Kinematic dynamo action in spherical Couette flow. Geophys Astro Fluid 106:681–700
Wicht J (2014) Flow instabilities in the wide-gap spherical Couette system. J Fluid Mech 738:184–221
Zimmerman D (2010) Turbulent shear flow in a rapidly rotating spherical annulus. PhD thesis, Digital Repository at the University of Maryland, University of Maryland, College Park, MD, USA
Zimmerman D, Triana S, Lathrop D (2011) Bi-stability in turbulent, rotating spherical Couette flow. Phys Fluids 23:065104
Zimmerman D, Triana S, Nataf H-C, Lathrop D (2014) A turbulent, high magnetic Reynolds number experimental model of earth's core. J Geophys Res 119:4538–4557